$= 0$. We see that Q/K is the analog of the supersaturation ratio, while ln Q/K is the supersaturation defined according to (C3) from which one obtains Equation (17):

$$\ln Q = \ln K + \sigma \tag{17}$$

The form of the dependence of J, the crystal growth rate, on supersaturation is the province of crystal growth theory, as discussed by Mandel (*5*). Thermodynamically, we have only that $J = 0$ when $\sigma = 0$ and that the sign of J must be equal to that of σ.

Manuscript received February 21, 1966; revision received May 13, 1966; paper accepted May 16, 1966. Paper presented at A.I.Ch.E. Dallas Meeting.

Physical and Chemical Absorption in Two-Phase Annular and Dispersed Horizontal Flow

CHARLES E. WALES

Purdue University, Lafayette, Indiana

Overall mass transfer coefficients for physical desorption and chemical absorption of carbon dioxide in annular and dispersed two-phase flow in a 1-in. horizontal pipe have been measured. These coefficients have been correlated with gas and liquid flow rates and with the normality of the sodium hydroxide solutions used.

A new method of analysis was used to separate overall coefficients into individual gas and liquid film coefficients. Penetration theory equations were used to calculate the effective interfacial surface area and the penetration contact time. Changes in these variables have been explained in terms of the changes in flow pattern.

Annular and dispersed two-phase flow appear to offer an excellent vehicle for mass transfer. Both the liquid and the gas phases are in turbulent flow and the surface area of the dispersed liquid phase is very high. Research in concurrent gas-liquid flow has been directed primarily toward understanding and correlating pressure drop, holdup, and entrainment. A comparatively limited number of mass transfer studies have been reported (*1* to *3*, *18*).

TWO-PHASE FLOW THEORY

This work is a study of liquid phase controlled mass transfer in annular and dispersed two-phase flow in a horizontal 1-in. pipe. In annular flow some of the liquid is entrained but a majority of it is turbulently pushed along the wall. In dispersed flow a majority of the liquid is entrained as droplets. An increase in either the gas or liquid flow rate can bring about the transition from annular to dispersed flow.

Both pressure drop and holdup in two-phase flow have been correlated with the pressure drop of each phase flowing alone (*14*). In the range of variables involved in this work, the holdup is related to the mass flow rates and the specific volume of the gas by

$$R_L = \phi' \frac{(L)^{2/3}}{(G)^{2/3}(\bar{V})^{1/3}} \tag{1}$$

The amount of entrained liquid has been correlated with the volume flow rate of the liquid and gas and the critical Weber number (*10*).

$$E = \phi'' \frac{Q_L Q_G}{N_{We}} \tag{2}$$

Gas flow rates of 150 to 300 lb./hr. and liquid flow rates of 500 to 2,500 lb./hr. were used in this work. The change in flow pattern produced by the change in either flow rate can be expected to result in a change in the turbulence in both phases and a change in the interfacial surface area, the penetration contact time, the liquid film coefficient, and the gas film coefficient.

PENETRATION MASS TRANSFER THEORY

In 1935 Higbie (*11*) proposed the penetration model for mass transfer in the liquid phase. Unsteady state molecular diffusion begins when a macroscopic element of the fluid is exposed to the gas phase. As long as the liquid element remains undisturbed, the solute continues its peneration of the stagnant surface film. Because a constant driving force is applied to an ever increasing depth of penetration, the initially high rate of mass transfer decreases. If this unsteady state process continues uninterrupted for a sufficient length of time, Whitman's steady state film model becomes applicable. However, Higbie proposed that the penetration process would be interrupted before steady state was reached by turbulent eddies which bring fresh elements of liquid from the core to the surface. The equation that describes this process for physical absorption is

$$k_L a^o = 2a\sqrt{\frac{D_A}{\pi T}} \qquad (3)$$

Danckwerts (*4*) modified Higbie's model, but calculations (*8*) have shown that both models give essentially the same result. The peneration theory equations for physical absorption have been verified by several experimenters (*13, 15, 16*).

CHEMICAL MASS TRANSFER THEORY

Diffusion through the liquid film is usually the controlling step in the mass transfer process. To increase the rate of mass transfer, a chemical which reacts with the solute is added to the liquid phase. In this work sodium hydroxide solutions were used to increase the rate of absorption of carbon dioxide from air. When the inequality $\sqrt{D_A k_r (\mathrm{OH})_o}/k_L^o >> 1 + C^*/(\mathrm{OH})_o$ is satisfied, a pseudo first-order reaction occurs (*5, 15, 16*). Danckwerts (*5, 8*) has shown that when a pseudo first-order reaction takes place, the liquid film coefficient can be predicted by

$$(k_L a)^2 = a^2 D_A k_r (\mathrm{OH})_o + \frac{4a^2 D_A}{\pi T} \qquad (4)$$

When $k_r(\mathrm{OH})_o >> \frac{4}{\pi T}$, Dankwerts' model, Higbie's model, and the Whitman film model all give the same result, which is

$$k_L a = a\sqrt{D_A k_r (\mathrm{OH})_o} \qquad (5)$$

When a pseudo first-order reaction occurs, $k_L a$ is independent of both contact time and the concentration of carbon dioxide. Equation (5) has been verified experimentally (*15*).

SURFACE AREA AND PENETRATION CONTACT TIME

Danckwerts (*8*) has verified Equation (4) and has shown that mass transfer coefficients for a system in which a chemical reaction takes place may be used to determine the effective interfacial surface area and the contact time. The graph of Equation (4) with $(k_L a)^2$ as ordinate and $D_A k_r (\mathrm{OH})_o$ as abscissa is a straight line with a slope equal to a^2. By using the value of effective interfacial area thus determined and the intercept of the line, it is possible to calculate the penetration contact time T. Danckwerts and Roberts (*7*) measured the chemical absorption of carbon dioxide in a packed tower. Equation (4) was used to determine values of a and T, which were used to predict the mass transfer coefficients for the physical absorption of carbon dioxide in sodium chloride solutions. Experimental data from the tower verified the calculations.

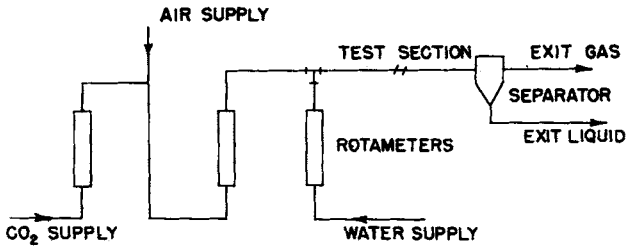

Fig. 1. Experimental equipment.

EXPERIMENTAL EQUIPMENT

Mass transfer rates in two-phase annular and dispersed flow were measured with the equipment shown in Figure 1. The test section was a horizontal tube 24 ft. long, constructed by joining 6-ft. lengths of 1-in. I.D. extruded polymethylmethacrylate tubing. Negligible flow disturbance resulted from the cemented joints.

The entrance section was a standard 1-in. screwed pipe tee connected on the run to the test section. Water (or sodium hydroxide solution) was drawn from a storage tank by a centrifugal pump which forced it through a calibrated rotameter and into the side entrance of the mixing tee. The water entered the tee from directly below and at a right angle to the test section, because this arrangement has been shown to produce higher entrainment and a lower pressure drop (*10*).

Carbon dioxide was supplied by a standard carbon dioxide cylinder. The high pressure carbon dioxide was heated to avoid the formation of the solid phase during decompression. The pressure was reduced to 35 lb./sq.in.gauge by a standard gas regulator before the gas was passed through a calibrated rotameter and mixed with air from the building supply. This mixture was metered and fed to the mixing tee.

The test section contained two sample probes located 16 ft. apart. The first probe was 7 ft. downstream from the mixing tee, far enough downstream to eliminate entrance effects (*1*). A probe consisted of a ¼-in. polyflow tube cut off at a 45-deg. angle. This was inserted through the bottom of the pipe facing upstream with the tip of the probe at the centerline of the pipe. Each probe was connected to a receiver below the test section. Each receiver was in turn connected to a pressure gauge and back to the system. This arrangement allowed the sample to be collected and withdrawn under the pressure of the system. This was especially important during the work with pure water to prevent the loss of carbon dioxide from the sample.

EXPERIMENTAL PROCEDURE

A series of desorption runs was started by saturating pure water in the feed tank with carbon dioxide. The air was turned on and then the water. Flow rates and the pressure were adjusted to the desired level, samples were taken, and the levels were changed. A liquid sample was collected by allowing it to flow slowly down through capillary tubing and up through a 25-cc. pipette, overflowing into a test tube which was connected back to the system. After approximately 50 cc. had passed through the pipette, flow was stopped, and a 25-cc. sample was withdrawn into a measured quantity of standardized barium hydroxide in a test tube. Samples were titrated with standardized hydrogen chloride with a pH meter to determine the end-point.

Sodium hydroxide solutions were also collected with the water receiving system. However, because there was no danger of the carbon dioxide escaping from the sodium hydroxide solution as there had been with water, the system was redesigned to allow both gas and liquid to flow directly into the receiver. Measurements from the two receiver systems were comparable. The liquid accumulated in the receiver test tube while the gas recycled back to the system. About 50 cc. of liquid were discarded before flow was stopped and the 25-cc. sample was withdrawn into a test tube. An excess of barium chloride was added to each sample to precipitate the carbonate anion as barium carbonate. Samples were titrated with stand-

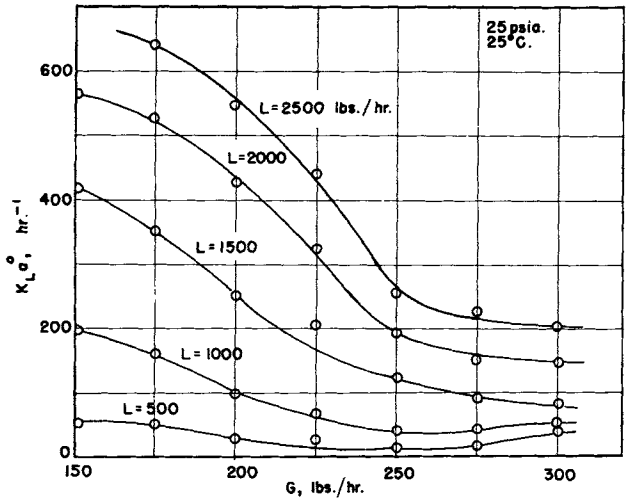

Fig. 2. Physical desorption. Effect of gas and liquid flow rates on the overall coefficient $K_L a^o$.

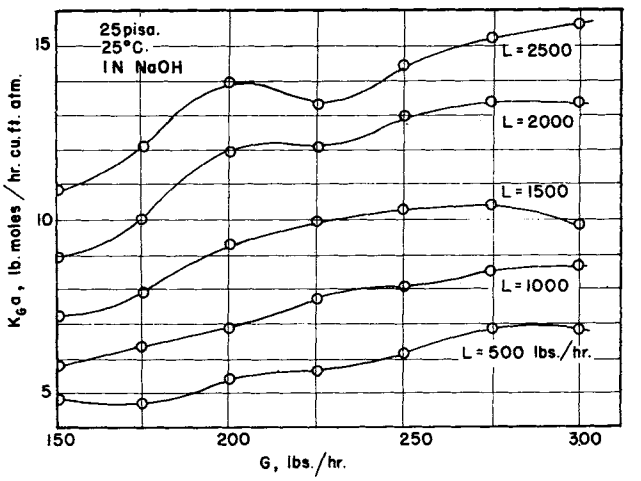

Fig. 3. Chemical absorption. Effect of gas and liquid flow rates on the overall coefficient $K_G a$.

ardized hydrogen chloride to a phenolphthalein end point. Total sodium normality was determined by titration with methyl orange as the indicator.

RESULTS AND DISCUSSION

Values of the overall coefficient for physical absorption were calculated with the equation

$$K_L a^o = \frac{L\,\Delta x}{(C^* - C_o)V} \qquad (6)$$

Because there was essentially no carbon dioxide in the gas phase, $y_o = 0$ and $C^* = 0$. The effects of changes in liquid and gas rates on the overall coefficient $K_L a^o$ are shown in Figure 2. Bollinger (3) reports K_L^o data for this system in annular flow with comparable liquid flow rates but lower gas flow rates. When these K_L^o data are multiplied by the constant annular area used by Bollinger, the resulting $K_L a^o$ data are in substantial agreement with those reported here.

Mass transfer in this system is liquid film controlled. As the gas flow rate increases, the flow pattern changes from annular to dispersed flow, the entrainment increases, the surface area for mass transfer increases, but the holdup decreases. The entrained droplets move at a velocity near that of the gas and as a result the turbulence in the liquid film of the droplets should be lower than that of the annular liquid. This effect apparently offsets the increase in the surface area and $K_L a^o$ falls as the gas rate increases. This reasoning will be supported later by calculated values of surface area, liquid film coefficient, and penetration contact time.

When the liquid flow rate is increased, the entrainment, the holdup, and the surface area increase. A thicker, more turbulent annular film is apparently produced and $K_L a^o$ increases. Equations (1) and (2) show that increased system pressure increases the holdup and decreases the entrainment. As a result, a pressure increase produces a significant increase in the overall coefficient (*19*). These data have been corrected to an average test section pressure of 25 lb./sq. in. abs. The usefulness of physical absorption in concurrent flow is limited by equilibrium, but if two-phase flow is used the highest physical mass transfer coefficients occur in annular flow.

Values of the overall coefficient for chemical absorption were calculated with the equation

$$K_G a = \frac{L\,\Delta x}{(y_o - y^*)PV} \qquad (7)$$

Because the carbon dioxide which enters the liquid reacts with the sodium hydroxide, C_o is zero and $y^* = 0$. The overall coefficient is reported in terms of $K_G a$ because it has been common practice in the past to report data for this system in these units (*9, 12*). Stutzman (*18*) has reported $K_G a$ data for concurrent two-phase flow in a packed tower. While it is not possible to make a direct comparison between a packed tower and the horizontal pipe used in this work, it is worth noting that Stutzman's coefficients are the same order of magnitude as those reported here.

Although a significant gas film resistance does exist in this system, mass transfer is liquid film controlled. For the concentrations of carbon dioxide and sodium hydroxide used in this work, the reaction in the liquid phase is pseudo first-order. Equation (5) shows that when a pseudo first-order reaction occurs neither turbulence in the liquid film nor penetration contact time affect the liquid film coefficient. Therefore, in this system the interfacial surface area plays the dominant role and the sodium hydroxide concentration sets the level at which it operates. The effect of liquid and gas rates on $K_G a$ is shown in Figure 3. Data for 0.1, 0.5, and 1.5 N solutions show similar patterns (*19*). Because the surface area is highest in dispersed flow, this pattern produces the highest mass transfer coefficients in a chemical absorption system.

As the gas flow rate increases and the flow changes from annular to dispersed, more of the liquid is entrained and the holdup is reduced. As entrainment increases, the sur-

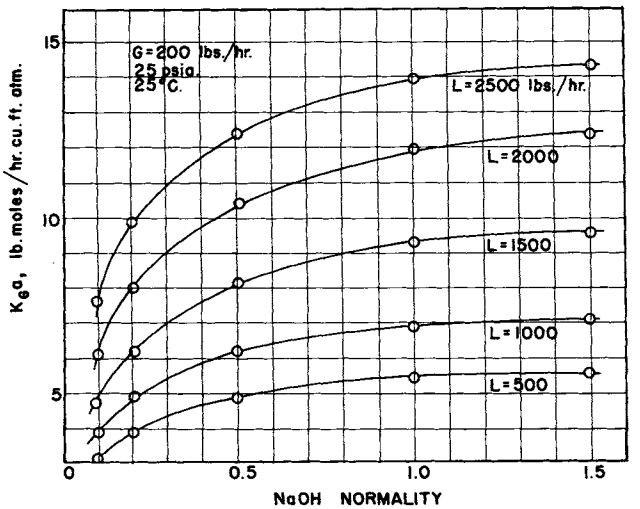

Fig. 4. Effect of sodium hydroxide normality on the overall coefficient $K_G a$.

face area increases and K_Ga increases. As the liquid flow rate increases, entrainment, holdup, and surface area increase and K_Ga increases. An increase in the system pressure reduces the entrainment and the surface area and K_Ga decreases. The gas composition was varied from 1.4 to 4.5% carbon dioxide with no apparent effect on the value of K_Ga. Sodium hydroxide normality was varied from 0.05 to 1.5 N. These concentrations are well above those necessary to ensure a pseudo first-order reaction (*6*). The conversion of sodium hydroxide to the carbonate ranged up to 30% but these data have been corrected to approximately 0% conversion by using data reported in the literature (*9, 12*).

Figure 4 shows an example of the effect of sodium hydroxide normality on K_Ga. The overall coefficient increases until a normality between 1.5 and 2 is reached and then the coefficient begins to fall off. This is the same effect noted in other experimental work. It has been attributed to the increase in the viscosity of the solution (*9*).

PREDICTION OF FILM COEFFICIENTS AND SURFACE AREA

These data suggest a method of analysis which makes it possible to separate the overall coefficient into individual gas and liquid film coefficients. It is assumed that neither the gas film coefficient nor the flow pattern is affected by changes in sodium hydroxide concentration below 1.5 N. Danckwerts (*5*) has confirmed that the series resistance concept, Equation (8), is still valid with penetration theory analysis:

$$\frac{1}{K_Ga} = \frac{H}{k_La} + \frac{1}{k_Ga} \qquad (8)$$

This equation is combined with Equation (5), which relates the liquid film coefficient to the properties of the solution, to give

$$\frac{1}{K_Ga} = \frac{1}{a}\frac{H}{\sqrt{D_Ak_r(\mathrm{OH})_o}} + \frac{1}{k_Ga} \qquad (9)$$

Values of k_r and D_A, and corrections for the effect of sodium hydroxide concentration were taken from the literature (*15, 16*). Values of H were also taken from the literature (*17*) and checked experimentally. These values were corrected for sodium hydroxide concentration by using the saturation concentration of the gas reported in reference *15*. The values used in this calculation may be determined by using the equations shown in Table 1.

Figure 5 shows how the data fit the relationship predicted by Equation (9). The gas film coefficient k_Ga is equal to the reciprocal of the intercept of each line. The interfacial surface area is equal to the reciprocal of the slope. These lines were determined by a least squares fit of the data with an IBM 7094 computer.

INDIVIDUAL FILM COEFFICIENTS

The values of interfacial surface area determined with Equation (9) are shown in Figure 6. These curves follow the pattern predicted earlier. Values of k_Ga determined with Equation (9) were divided by the corresponding area values to determine the values of the gas film coefficient k_G shown in Figure 7. As shown k_G decreases with increasing gas flow rate. This may be explained by recalling that as the gas flow rate increases, the entrainment also increases. Increased entrainment results in lower relative velocities between the gas and the entrained liquid phase. With less turbulence in the gas film around the entrained droplets, the gas film coefficient k_G can be expected to decrease as it does. This is of course directly opposite to the effect in countercurrent flow, where an increased gas flow rate results in higher turbulence and an increased gas film coefficient.

TABLE 1. EQUATIONS FOR PROPERTIES

$$D_A = 1.833 \times 10^{-6}T - 4.717 \times 10^{-4} - 1.042 \times 10^{-5}\mathrm{N}$$

$$\log H = 0.149\,\mathrm{N} + \log\,(15.4T - 3996.2)$$

$$\log k_r' = \frac{-3.56 \times 10^3}{T} + 15.8494 + 0.1315\,\mathrm{N}$$

where T = °K., k_r' = cu. ft./(lb.-mole)(sec.), H at 25 lb./sq. in. abs.

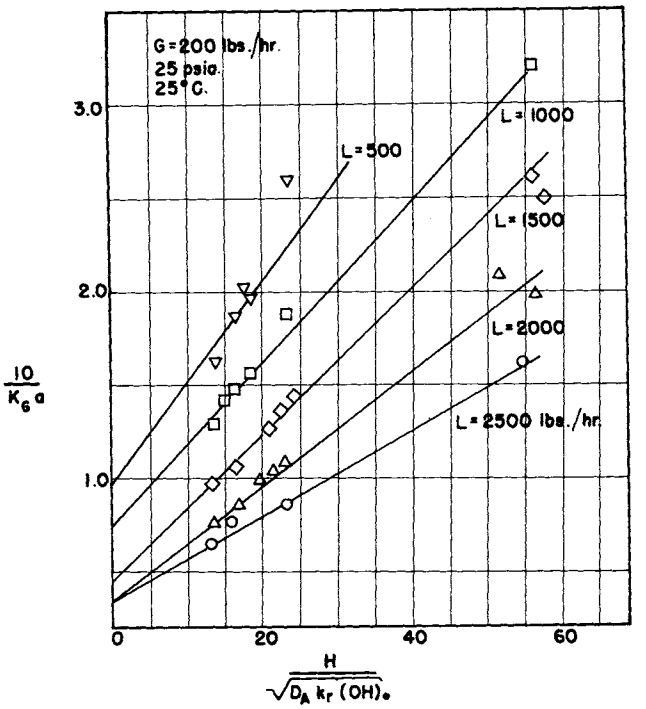

Fig. 5. Regression lines used to predict k_Ga and a.

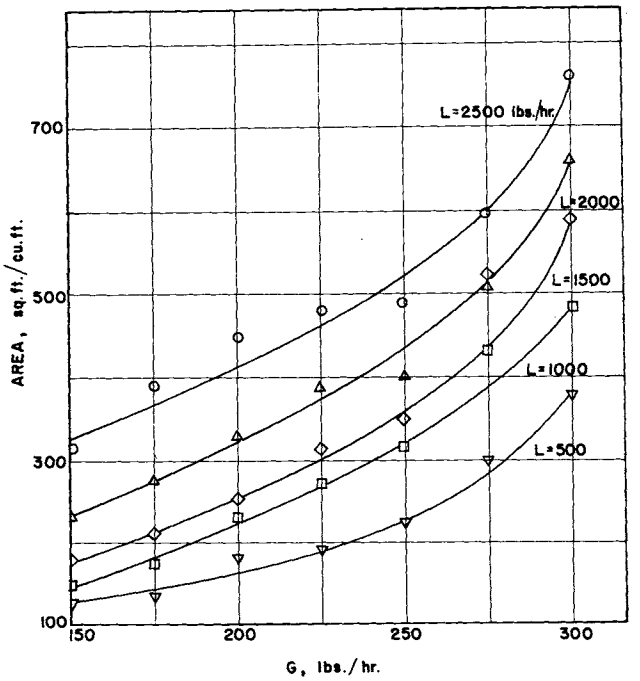

Fig. 6. Effect of gas and liquid flow rates on the interfacial surface area.

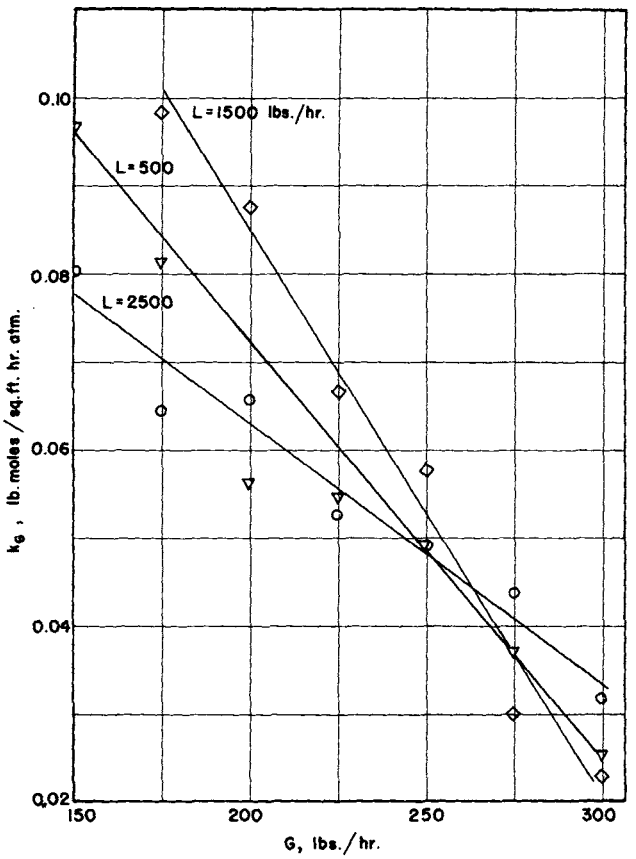

Fig. 7. Effect of gas and liquid flow rates on the gas film coefficient k_G.

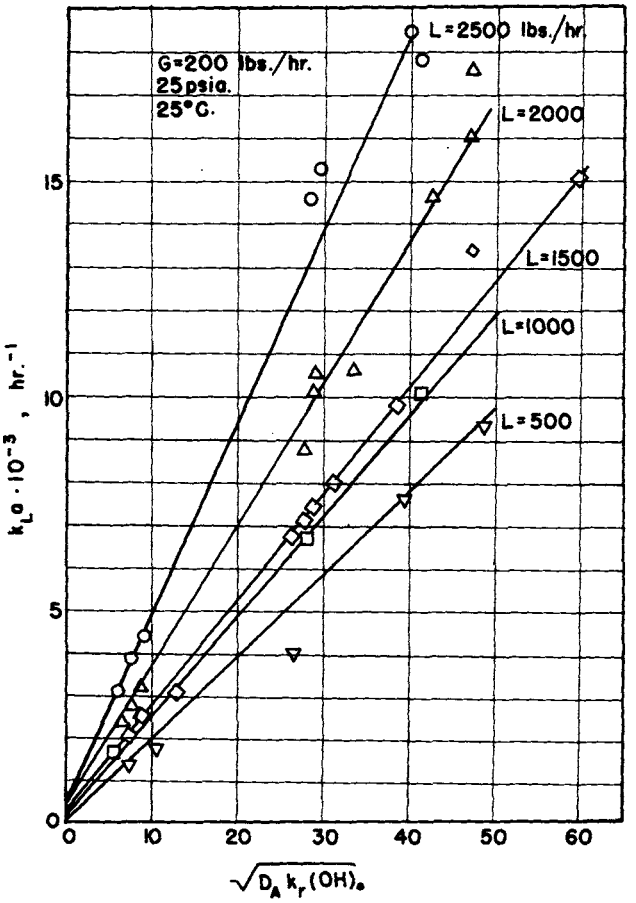

Fig. 8. Penetration theory determination of area.

Figure 7 also shows that k_G is increased by increasing the liquid flow rate from 500 to 1,500 lb./hr. Higher liquid rates result in increased holdup, which reduces the area for gas flow. This in turn produces higher gas velocities, and increased gas film coefficients are expected. At liquid flow rates between 1,500 and 2,500 lb./hr., the flow pattern apparently changes from annular to dispersed and k_G decreases. It should be noted that these values of k_G do not agree with the values of K_G for ammonia absorption reported by Anderson, Bollinger, and Lamb (2). Their work is based on a constant annular area but after the data are corrected for this assumption, their values of K_G are still greater than these values of k_G by a factor of 10 to 100. The effect of pressure is not mentioned in their paper, but it does not seem likely that this correction will account for all of this large difference.

In physical absorption the gas film resistance is small compared to the liquid film resistance. Therefore, $K_L a^o$ is approximately equal to $k_L a^o$ and the value of the liquid film coefficient k_L^o may be calculated by dividing values of $k_L a^o$ by the effective interfacial area. At a gas flow rate of 150 lb./hr. and a liquid flow rate of 500 lb./hr., entrainment is low and holdup is high. Most of the liquid is in the annular film and k_L^o has a value of 0.55 ft./hr. When the gas rate is increased to 300 lb./hr. essentially all of the liquid are entrained and the value of k_L^o falls to 0.048 ft./hr.

When the gas flow rate is 150 lb./hr. and the liquid rate is increased to 2,500 lb./hr., the annular film is thicker and more turbulent and the value of k_L^o is 2.16 ft./hr. When the gas rate is increased to 300 lb./hr. the thickness and turbulence of the annular liquid are decreased and k_L^o is reduced to 0.27 ft./hr. These results support the earlier conclusions concerning the importance of turbulence in the annular film to physical mass transfer.

PENETRATION THEORY PREDICTION OF SURFACE AREA

The effective interfacial surface area was determined with Equation (9). It may also be determined with the penetration theory, Equation (4). In this work, the left side of the inequality $\sqrt{D_A k_r (OH_o)}/k_L^o >> 1 + C^*/(OH)_o$ varies from 2.3 to 5,000; the ratio is above 10 for almost all the data. Because $(OH)_o >> C^*$, the right side of the equation is equal to one and the inequality is satisfied. When chemical absorption occurs, the value of the second term on the right is negligible and Equation (4) reduces to Equation (5). When the hydroxyl ion concentration is zero, the first term on the right is zero and Equation (4) reduces to Equation (3).

Values of $k_L a$ were determined with Equation (10) by using measured $K_G a$ data and the values of $k_G a$ previously calculated.

$$k_L a = \frac{H}{\frac{1}{K_G a} - \frac{1}{k_G a}} \qquad (10)$$

As predicted, the relationship between $k_L a$ and the square root of the group $D_A k_r (OH)_o$, Equation (5), is a straight line, Figure 8. The intercept of each line represents the physical absorption coefficient for the given conditions, Equation (3). The experimental values of the physical absorption coefficient $K_L a^o$, shown in Figure 2, are predicted by these lines. This fact supports the accuracy of these data and this method of analysis.

The slope of each line in Figure 8 represents an effective interfacial surface area. The values of surface area calculated with Equation (5) agree with the values calculated with Equation (9), which is a further check on the adequacy of equations used.

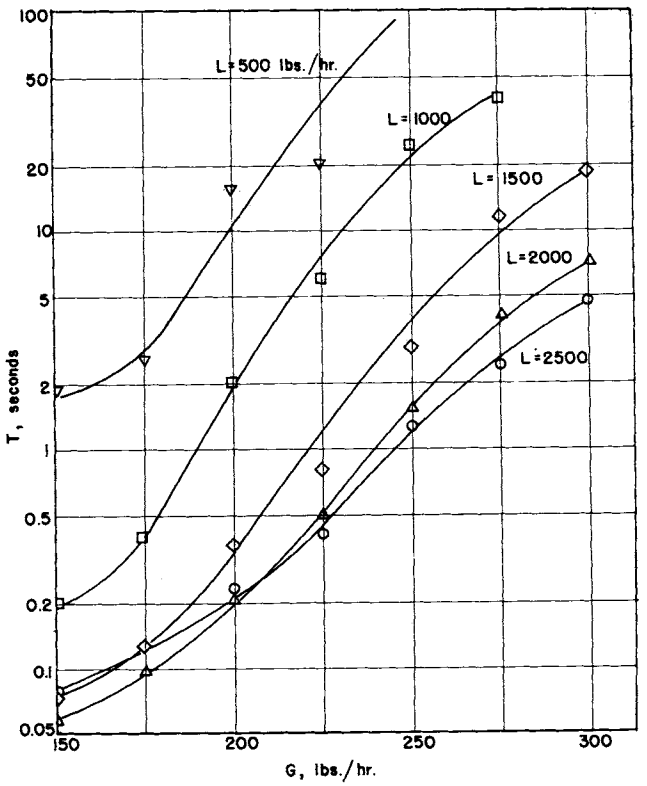

Fig. 9. Effect of gas and liquid flow rates on the penetration contact time.

PREDICTION OF CONTACT TIME

Values of the effective interfacial surface area from Figure 6 and the corresponding values of K_La^o for the water experiments were combined in Equation (3) for physical absorption to calculate the penetration contact time. Calculated values of contact time are shown in Figure 9. This figure confirms the predictions made earlier for physical absorption. As the liquid flow rate is increased, the holdup is increased, the gas velocity is increased, annular turbulence is increased, and the contact time decreases. When the gas velocity is increased, more of the liquid is entrained. Because the relative velocity of the liquid phase is reduced, droplet turbulence is reduced and the contact time increases.

USE OF AREA AND CONTACT TIME

The values of effective interfacial area and contact time that have been determined should apply to any gas-liquid system which has similar physical properties. Thus, these values may be combined with a value of molecular diffusivity in Equation (3) for physical absorption to predict the liquid film coefficient for the absorption of other gases in two-phase flow. The values of surface area may also be used with Equation (4) for chemical absorption to predict the liquid film coefficient for other systems in which a first-order reaction occurs.

ACKNOWLEDGMENT

The author extends his thanks to Purdue University, The Ford Foundation, and the American Oil Company whose financial support made this work possible. The counsel provided by Dr. Alden H. Emery is gratefully acknowledged.

NOTATION

a = effective interfacial surface area, sq. ft./cu. ft.
C_o = bulk concentration of the solute in the liquid phase, lb.-moles/cu. ft.
C^* = equilibrium concentration of the solute in the liquid phase, lb.-moles/cu. ft.
D_A = molecular diffusivity of the solute in the solvent, sq. ft./hr.
E = pounds of the liquid phase entrained
G = mass flow rate of the gas phase, lb./hr.
H = Henry's law constant, (atm.) (cu. ft.)/lb.-mole
k_G = gas film mass transfer coefficient, lb.-moles/(atm.) (hr.) (sq. ft.)
k_Ga = gas film mass transfer coefficient, lb.-moles/(atm.) (hr.) (cu. ft.)
K_Ga = overall mass transfer coefficient, lb.-moles/(atm.) (hr.) (cu. ft.)
k_L = liquid film mass transfer coefficient, ft./hr.
k_La = liquid film mass transfer coefficient, 1/hr.
K_La = overall mass transfer coefficient, 1/hr.
k_r = reaction rate constant, cu. ft./(lb.-moles) (hr.)
L = flow rate of the liquid phase lb./hr. or lb.-moles/hr.
N_{We} = critical Weber number
$(OH)_o$ = initial concentration of the hydroxyl ion, lb.-moles/cu. ft.
P = system pressure, atm.
Q_L = volume flow rate of the liquid phase, cu. ft./hr.
Q_G = volume flow rate of the gas phase, cu. ft./hr.
R_L = fraction of the pipe filled by the liquid phase
T = contact time of the two phases, sec. or hr.
V = volume of the mass transfer equipment, cu. ft.
$\bar{V}$ = specific volume of the gas phase, cu. ft./lb.
Δx = change in concentration of carbon dioxide in the liquid phase
y_o = mole fraction in the bulk gas phase
y^* = equilibrium mole fraction in the gas phase

Superscript

o = physical absorption coefficient

LITERATURE CITED

1. Anderson, J. D., M.S. thesis, Univ. Delaware, Newark (1959).
2. ———, R. E. Bollinger, and D. E. Lamb, *A.I.Ch.E. J.*, 640 (1964).
3. Bollinger, R. E., M.S. thesis, Univ. Delaware, Newark (1960).
4. Danckwerts, P. V., *Trans. Faraday Soc.*, **46**, 300 (1950).
5. ———, *A.I.Ch.E. J.*, **1**, 456 (1955).
6. ———, and A. M. Kennedy, *Chem. Eng. Sci.*, **8**, 201 (1958).
7. Danckwerts, P. V., and J. D. Roberts, *ibid.*, **17**, 961 (1962).
8. Danckwerts, P. V., G. A. Ratcliff, and G. M. Richards, *ibid.*, **19**, 325 (1964).
9. Dodge, B. F., and J. B. Tepe, *Trans. Am. Inst. Chem. Engrs.*, **39**, 255 (1943).
10. Duckler, A. E., and Moye Wicks III, *A.I.Ch.E. J.*, **6**, 463 (1960).
11. Higbie, Ralph, *Trans. Am. Inst. Chem. Engrs.*, **31**, 365 (1935).
12. Leva, Max, *A.I.Ch.E. J.*, **1**, 224 (1955).
13. Lynn, S., R. J. Straatemeier, and H. Kramers, *Chem. Eng. Sci.*, **4**, 49 (1955).
14. Martinelli, R. C., and R. W. Lockhart, *Chem. Eng. Progr.*, **45**, 39 (1949).
15. Nijsing, R.A.T.O., R. H. Hendriksz, and H. Kramers, *Chem. Eng. Sci.*, **10**, 88 (1959).
16. Rehm, T. R., A. J. Moll, and A. L. Bass, *A.I.Ch.E. J.*, **9**, 760 (1963).
17. Seidell, A., and W. F. Linke, "Solubilities," 4 ed., p. 459, Van Nostrand, N. J. (1958).
18. Stutzman, B. J., W. S. Dodds, B. J. Sollami, and R. J. McCarter, *A.I.Ch.E. J.*, **6**, 197 (1960).
19. Wales, C. E., Ph.D. thesis, Purdue Univ., Lafayette, Ind. (1965).

Manuscript received August 10, 1965; revision received May 9, 1966; paper accepted May 13, 1966.